Cluster Routing-Based Data Packet Backhaul Prediction Method in Vehicular Named Data Networking

Rui Hou, *Member, IEEE*, Shuo Zhou, Yong Zheng, Mianxiong Dong, *Member, IEEE*, Kaoru Ota, *Member, IEEE*, Deze Zeng, *Member, IEEE*, Jiangtao Luo, *Senior Member, IEEE*, and Maode Ma, *Senior Member, IEEE*

***Abstract*—Vehicular named data networking (V-NDN) is a network architecture that combines named data networking (NDN) and vehicular ad hoc networks (VANETs). Due to the high-speed mobility of the on-board unit (OBU) in V-NDNs, topological changes may cause the problem of reverse path breaking for data packets, thus impacting the communication quality of service (QoS) among vehicles. To address this issue, a data packet backhaul prediction method (DBPM) based on cluster routing in the V-NDN is proposed in this paper. The DBPM uses GPS and a convex programming location algorithm (CPLA) at roadside units (RSUs) to obtain the positioning information of vehicle in the clusters, and uses two positioning data items to predict the location of the vehicle's future access point (AP) for the cluster by using the Kalman filtering model. Then, the DBPM forwards the returned data packets to the vehicle by the cluster. Simulation experiments are performed by using the simulators Simulation of Urban Mobility (SUMO) and VanetMobiSim. Results show that the proposed DBPM can effectively reduce the average delay and packet loss ratio in the vehicle-to-infrastructure (V2I) communication in urban scenes, thus enhancing the robustness of data transmission and effectively supporting the data communication's QoS of V-NDN.**

***Index Terms*—Vehicular ad hoc network, Named data networking, Kalman filtering, Convex programming location algorithm, quality of service.**

I. Introduction

With the development of internetworking technology, the combination of vehicles and internet technology has greatly promoted the efficiency of vehicle communication. The vehicular ad hoc network (VANET) is an application of the mobile ad hoc network (MANET) in the transportation field [1]. Currently, the role of VANET has become increasingly important in smart city construction. However, due to its dynamic network topology and high-speed vehicle mobility, etc., seamless data communications of vehicle-to-infrastructure (V2I) and vehicle-to-vehicle (V2V) in VANETs has become a developmental bottleneck considering QoS support [2].

Named data networking (NDN) is one of the implementations of information-centric networking (ICN). It has an information object's name-based networking architecture that can decouple an information object with its location [3]. The NDN has transferred the address-based routing mode in the IP-based networks to the information object's name-based data searching mode, and it has been regarded as a clean-slate network architecture for the future internetworking.

In recent years, to adapt to the networking development trend, a novel vehicular networking paradigm was introduced: vehicular named data networking (V-NDN). It combines the attributes and features of VANETs and NDNs [4]–[7]. In the conventional IP-based Internet architecture, data packets' routing and transportation layer connections are restricted by the nodes' mobility because the IP address changes with the node's location, which increases network overhead and end-to-end delays and interrupts data transmission.

Similar to the NDN, a V-NDN assigns a specific name for identifying each information object (e.g., a movie or a photo) and uses the name-based packets' routing approach. It converts the data communication approach from the host-centric end-to-end data communication mode to the information-centric subscriber/publisher data exchange mode, which decouples data transmission and its geographic location [8]. With such characteristics, the V-NDN can fetch the requested information object more quickly and more effectively, thus

Manuscript received December 21, 2020; revised June 29, 2021; accepted August 2, 2021. Date of publication August 6, 2021; date of current version September 16, 2021. This work was supported in part by the National Natural Science Foundation of China under Grant 61972424, in part by JSPS KAKENHI under Grants JP16K00117 and JP19K20250, in part by the Leading Initiative for Excellent Young Researchers (LEADER), MEXT, Japan, and KDDI Foundation, and in part by the Special Fund for Basic Scientific Research of Central College, SCUEC under Grant CZT20025. Recommended for acceptance by Dr. Yan Zhang. *(Corresponding author: Rui Hou.)*

Rui Hou, Shuo Zhou, and Yong Zheng are with the College of Computer Science, South-central University for Nationalities, Wuhan 430074, Hubei, China (e-mail: hourui@mail.scuec.edu.cn; zhoushuo_stu@163.com; smile_luffy@126.com).

Mianxiong Dong is with the Department of Information and Electronic Engineering, Muroran Institute of Technology, Muroran, Hokkaido 050-8585, Japan (e-mail: mx.dong@csse.muroran-it.ac.jp).

Kaoru Ota is with the Department of Information and Electronic Engineering, Muroran Institute of Technology, Muroran, Hokkaido 050-8585, Japan (e-mail: ota@csse.muroran-it.ac.jp).

Deze Zeng is with the School of Computer Science, China University of Geosciences, Wuhan 430074, Hubei, China (e-mail: deze@cug.edu.cn).

Jiangtao Luo is with the Electronic Information and Networking Research Institute, Chongqing University of Posts and Telecommunications, Chongqing 400065, China (e-mail: luojt@cqupt.edu.cn).

Maode Ma is with the School of Electrical and Electronic Engineering, Nanyang Technology University, Nanyang, Singapore 639798, Singapore (e-mail: emdma@ntu.edu.sg).

Digital Object Identifier 10.1109/TNSE.2021.3102969

promoting the efficiency of data exchange. However, the V-NDNs also face a reverse path breakage problem due to the high-speed mobility of OBUs by which data packets sent by the publisher OBU may fail to reach the subscriber OBU who has sent the corresponding interest packet. Therefore, ensuring that an OBU can reliably receive a data request at the previous OBU has been challenging in the research of V-NDN.

The rest of this paper is organized as follows: Section II provides an overview of related works. Details of cluster structure design in V-NDN are represented in section III. Section IV introduces the routing process of DBPM. In Section V, the prediction model of vehicle movement is introduced. Section VI presents an extensive simulation to demonstrate the performance efficiency of proposed DBPM. Finally, we conclude the article in section VII.

II. Related Work

To solve the problem of data link breakage due to the high mobility of OBUs, researchers in refs. [9]–[11] have mainly focused on native mobility support based on the mobility of subscriber, proxy-based mobility, rapid request retransmission recovery, and proactive caching. A distributed active caching method is proposed in [12], that uses a user's mobile information to determine the destination for actively cached content to realize seamless data transmission using a congestion pricing mechanism. In [13], an agent-based mobile support method named Proxy-based Mobility support approach for mobile NDN (PMNDN) is proposed which manages source migration through agents and caches to resolve communication outages.

A RSU assisted geocast (RAG) method is proposed in [14] for selecting the best next-hop RSU to forward packets to the destination. This method uses the quadtree model to decompose RSUs in the global domain, and a tree construction method to predict the location of nodes is used to determine the intersection of the destination area and the quadtree. However, the maintenance of the routing locations information of the quadtree will increase network overhead. A fuzzy-weighting location mechanism (FLM) is designed in [15] that combines GPS, Wi-Fi, and cellular network technology to dynamically adjust the measurement noise covariance to obtain a more accurate vehicle location information. In [16], a Kalman Prediction-based Neighbor Discovery (KPND) algorithm is proposed which can predict the mobility of a vehicle and its neighbors by using a Kalman filter mobility prediction model. The KPND algorithm uses position broadcast to enhance the prediction algorithm to achieve more efficient routing and data distribution.

A content-based convergence scheme is proposed in [17] to enhance NDNs' mobility, where mobile receivers can republish subscriptions for unreceive content when relocating and reconnecting to the V-NDN networks. Once the subscription is received, the center server calculates a new path between the subscriber and the publisher. In [18], a method for requesting redirection through the management routing table of interest packets is proposed which can implement efficient path replacement for failed nodes or paths in mobile scenarios.

A user mobility-supported scheme called Kite is proposed in [19], by which entries in the pending interest table (PIT) can be used to track the mobile node for group communication among mobile nodes. An entropy-based proactive strategy is proposed in [20] for estimating the uncertainty of the mobile prediction to preselect nodes and delete redundant buffers, thus reducing backhaul traffic and delay. However, this strategy may reduce the caching efficiency of edge nodes.

An IoT-Named Computation Networking (IoT-NCN) framework for data processing and forwarding at the edge nodes is proposed in [21]. This method can minimize the cost function between data requesters and IoT data that need to be processed, thus reducing the service provisioning time. A cluster-based cooperative caching approach with a mobility prediction (COMP) method is proposed in [22] that establishes communication between vehicles with similar mobility patterns and divides the vehicles into groups by mobility prediction with cooperative caching, thus enhancing the performance of data transmission.

Although the above methods are useful for solving the data transmission problem in the node mobile environment, they have some limitations. Maintaining the routing location and real-time maintenance of the node neighbor table increases the network overhead. Moreover, node handover, prediction separation are affected by complicated road conditions.

This paper proposes a cluster routing-based Data packet Backhaul Prediction Method (DBPM), which first establishes a cluster of RSUs between two road intersections, referred to as a tubular structure cluster, and uses GPS and the CPLA [23] to obtain the position information of the subscriber vehicle to predict the target RSU by the Kalman prediction model. Then the router forwards the corresponding data packets to the tubular cluster located by the prediction RSU. Finally, the RSU closest to the subscriber vehicle will send the data packets with the OBU identification back to the subscriber vehicle.

The main contributions of this paper are the following:

1) Cluster structure and clustered routing. Cluster topological nodes for V2I communication can be managed by the router and actively buffer the returned data packets into the cluster of future RSU predicted by the DBPM method. It can reduce the number of data packet routing hops and reduce the waste of content store (CS) storage space in the topology node.
2) Improved CPLA. The CPLA based on the dichotomy radius sensing is used to reduce the number of flood broadcasts during radius sensing. Real-time positioning data is used to form a vehicle motion trajectory.
3) Target RSU prediction method. Vehicle positioning data obtained by the CPLA can be used by the RSU for vehicle sensing and GPS positioning. The method of combining the prediction results obtained from the two-positioning data is used to improve the prediction accuracy of the target RSU.

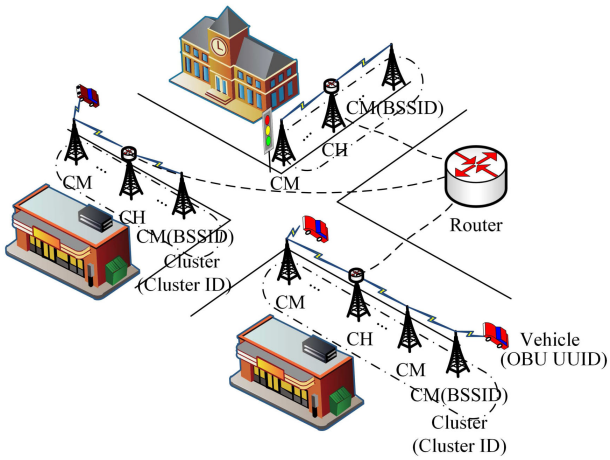

Fig. 1. Structure of a cluster.

TABLE I
CONNECTION STATUS TABLE

OBU UUID	The state bits of the RSUs		
	FBA7 8EFB CFF3	FBA7 8EFB CFF4	...
OBU UUID_1	1	1	0
OBU UUID_2	0	1	1
...	...	...	...

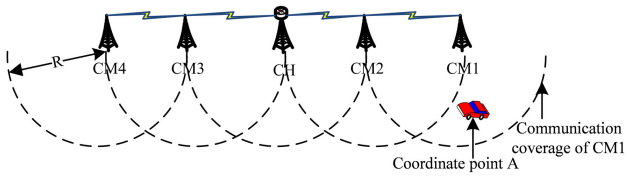

Fig. 2. Relationship between a vehicle and location of a cluster.

III. CLUSTER STRUCTURE DESIGN IN V-NDN

In the V-NDN, a subscriber obtains a data packet containing the corresponding request by sending an interest packet to routes [24]. When the data packet is returned along the original path, transmission instability or interruption may occur due to the subscriber's mobility, and the quality of communication may deteriorate. In this paper, a special cluster structure is set up through the kinematic relationship between moving vehicles and stationery RSUs to enhance V2I communication performance [25].

As shown in Fig. 1, a road is divided into multiple segments by considering the intersections as endpoints. Each RSU in a road segment is evenly arranged into clusters along the road. The RSU at the center of the road segment is used as the cluster head node (CH). There are at least three cluster members in each cluster. An edge router manages multiple adjacent clusters. This work will give an efficient solution to packet forwarding within the edge of V-NDN.

A. Connection State

The cluster ID is used as the unique identifier of the cluster to distinguish multiple clusters under the router. Each RSU in the cluster is uniquely identified by a 48-bit basic service set identifier (BSSID). Within the communication range of each cluster are a number of vehicles that are uniquely identified by the 128-bit OBU Universal Unique Identifier (UUID).

Each CH node maintains a connection status table, as shown in Table I, which records the connection status between a vehicle and cluster member (CM) in a cluster. The initial value of the connection state between the vehicle and the CM node is 0. When the vehicle is connected to a new CM, the vehicle sends a location update packet through CMs to the CH in the current cluster, which contains the OBU UUID of the current vehicle, location information, and the BSSID of the CM connected to the current vehicle. When the CH receives the corresponding packet, it immediately updates the connection status table. If the OBU UUID entry information exists in the table, then the status of the CM node is updated to 1. Otherwise, a new OBU UUID entry is added to the table.

For example, if the vehicle whose OBU UUID is OBU UUID_1 is moved from the RSU communication range with BSSID "FBA7 8EFB CFF3" to the RSU communication range of "FBA7 8EFB CFF4," then the status bits of the RSU nodes "FBA7 8EFB CFF3" to "FBA7 8EFB CFF4" change in the connection status table to 1, and the rest are 0.

Each cluster boundary is an intersection. Vehicles may enter from two intersections in the cluster corresponding to the RSU that changed the status bit first or last in the connection status table, and the remaining RSUs in the cluster are arranged in the order of road position in the connection state table. This is called the boundary node of each cluster according to the connection status table and can be determined from where the vehicle entered or left the cluster.

B. Relationship Between the Vehicle and Location of a Cluster

Each CH node stores the mapping relationship between the coordinate information of each RSU in the cluster and the current cluster ID. The cluster ID and RSUs have a one-to-many relationship. As shown in Fig. 2, the coordinate point A is known, and the RSU signal coverage is calculated from the RSU coordinates in the cluster-location table and their communication radius R. For example, when the coordinate point A is in the signal coverage of CM1, the coordinate point A is in the signal range of the cluster. Concurrently, the connection status table in the CH can also be used to determine whether the vehicle is in the cluster.

IV. CLUSTER ROUTING

When a subscriber moves in a cluster, it can send an interest packet through any RSU that communicates with it. If the subscriber receives its corresponding data packet from the same cluster, thus called intra-cluster communication. While if the subscriber leaves the cluster, and the data packet is delivered by another cluster is called inter-cluster communication.

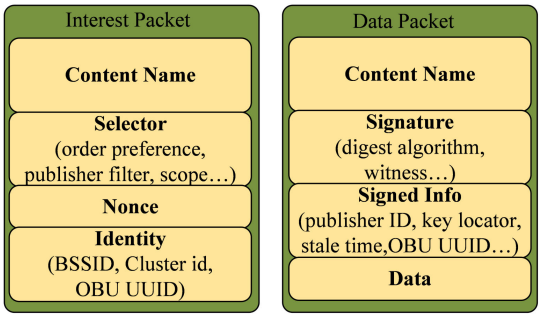

Fig. 3. Design of interest and data packets.

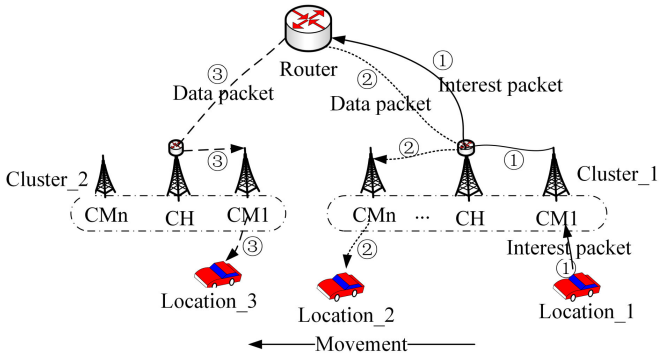

Fig. 4. Data packet flow.

A. Packet Format

As shown in Fig. 3, an identity field is added to the interest packet format in V-NDN, which includes the BSSID, cluster id, and OBU UUID. The OBU UUID information is also added to the Signed Info field of the data packet. When the interest packet finds the corresponding data in the CS of a router by name routing, the data will encapsulate into a data packet, and the OBU UUID information in the interest packet will be copied to the data packet.

After a subscriber sends an interest packet to its currently connected RSU, the Signed Info field of the returned data packet contains the OBU UUID information of the requested data. When the subscriber leaves out of the RSU's communication range, a new RSU node which it is connected will deliver the data packet according to the OBU UUID to the subscriber, and the data packet will be stored in the CS of the CH node to, so as to quickly satisfy the same subsequent requests.

For example, if the subscriber labeled OBU UUID_1 receives a data packet named "/com/yahoo/news/title.txt" in a cluster, then the data encapsulated in the data packet will be cached to the CS of the CH node. If the subscriber labeled OBU UUID_2 within the communication range of the same cluster also sends an interest packet named "/com/yahoo/news/title.txt," then the CH node encapsulates the corresponding data in its CS into a data packet and directly sends it to the subscriber, so that the subscriber labeled OBU UUID_2 does not need to get data from the source router any more but can receive the data packet nearby and quickly.

B. Communication Process

The interest packet sent by a subscriber is forwarded to the CH node via the CM node with which the subscriber communicates and is then routed through the router to obtain the corresponding data packet. The data packet will follow the reverse forwarding path of the interest packet and return to the corresponding cluster where the subscriber is located.

Since the subscriber is mobile during the data request process, the position of the subscriber will determine which cluster the data packet returns from the router. As shown in Fig. 4, the subscriber sends an interest packet at Location_1 in Cluster_1. The interest packet is forwarded along path_1 (①), and the CH node and router forward the interest packet to obtain the corresponding data packet. If the subscriber has moved from Location_1 to Location_2 within the communication range of Cluster_1 while waiting for the data packet, then the data packet arriving at the router will return to the CH of Cluster_1 according to path_2 (②), and the CH will deliver the data packet to the subscriber according to the information in the connection status table.

If the subscriber moves out of the scope of the communication range of the original cluster while waiting to receive the data packet and moves to the communication range of a new cluster, inter-cluster communication will be carried out at this time. As shown in Fig. 4, the subscriber will not receive the data packet when it leaves the boundary node CMn of Cluster_1 before receiving the data packet. At this time, the subscriber will send its current location information to the router, and the router will calculate the coordinates that the subscriber may reach after leaving the current cluster based on the updated position information. The specific routing algorithm is presented in Section III-C. The positional relationship between the subscriber and the cluster will be used to obtain the cluster that the subscriber is most likely to reach (Cluster_2), so that the router forwards the data packet to the CH node where Cluster_2 is located. Then, the CH node delivers the data packet to the subscriber along path_3 (③) according to the relevant entry in the stored connection status table.

C. Inter-Cluster Communication Algorithm Design

In V-NDN, the Pending Interest Table (PIT) records the input port or interface of an interest packet to enable its corresponding data packet to be returned along the reverse path of the interest packet. It is assumed that different clusters managed by an edge router correspond with different ports. As shown in Fig. 5, when a subscriber sends an interest packet to request the target data to the border node in Cluster_1 and does not receive the returned data packet when it is about to leave the cluster, it will send specific information including the subscriber location and OBU UUID to the router.

By adding the interface number corresponding to the cluster to the "incoming face" of the PIT in the router, its required data will be forwarded to the cluster that the subscriber will reach, so that the data packet can be successfully delivered to the subscriber according to path_2 (in Fig. 5 ②) in the updated PIT. Algorithm_1 describes the process in which the router predicts

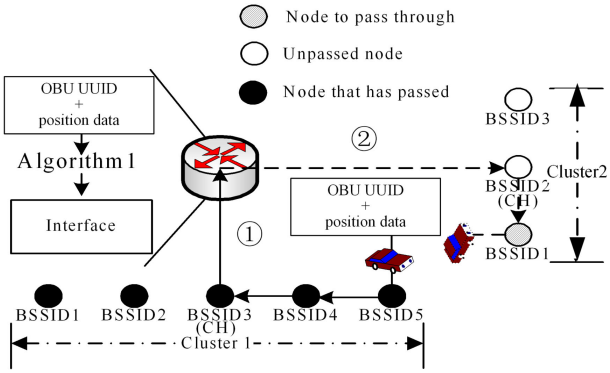

Fig. 5. Inter-cluster communication process.

TABLE II
PENDING INTEREST TABLE

Name	Incoming Faces
/com/amazon/sketch.pdf	face_1, face_2
/com/yahoo/news/title.txt	face_1
...	...

Algorithm 1. Predictive forwarding method

Input: (x, y, v, φ, a, W)
(x, y), Subscriber coordinates
v, Speed of vehicle
φ, Yaw angle
a, Acceleration of subscriber
W, Yaw velocity
Initialize:
Let the middle node of the cluster as Cluster Head (CH) initialize the Connection status table
Initialize PIT
while Router accepted Interest packet from subscriber **do**
if the RSU node with BSSID is the boundary RSU node **then**
upload the position data (x, y, v, φ, a, W) from subscriber
calculate the coordinate point by DBPM
compute the interface relevant to coordinate point
add interface into PIT
else
return the Data packet from Router to CH
deliver the Data packet by OBU UUID
end if
end while

the moving position of the subscriber and forwards the data. When the router calculates that the subscriber is about to arrive at Cluster_2, the interface corresponding to Cluster_2 is face_2. The packet named "/com/amazon/sketch.pdf" is sent from face_1 to the router. Then, face_2 is added to the incoming face of the PIT so that subscriber that is about to reach Cluster_2 can also receive the data packet requested by Cluster_1.

The PIT is shown in Table II. When the router calculates that the subscriber is about to reach Cluster_2, the interface corresponding to Cluster_2 is face_2. A data packet named "/com/amazon/sketch.pdf" is sent from face_1 to the router. The interface, face_2, is then added to the incoming faces of the PIT so that the subscriber that will reach Cluster_2 can also receive the data packet requested by Cluster_1.

Algorithm_1 includes the process of predicting the position of the next cluster to reach after leaving the cluster using both intra-cluster and inter-cluster communication. The predictive forwarding method is mainly divided into a position prediction process and data packet forwarding process. The time complexity of the data packet forwarding process is O(C), the time complexity of calculating AP in the prediction process is O(N), and the complexity of confirming the node state in the cluster is O (N). Thus, the time complexity of Algorithm_1 is O(N^2), where N is the scale of the problem and C is a constant.

V. PREDICTION MODEL

In urban conditions, the occlusion of GPS signals by tall buildings will increase coordinate errors [15], affect the prediction accuracy, and reduce the hit rate of the data packet. The RSU obtains positioning data through the CPLA [26] based on vehicle signal sensing, which is not affected by the GPS signal occlusion. At the same time, GPS can also obtain the vehicle positioning data.

The positioning data obtained by the GPS and CPLA described above are separately put into the Kalman prediction model. The two methods are combined to improve the accuracy and the stability of inter-cluster switching, yielding an exact return of the data packet in complex situations.

A. Convex Programming Location Algorithm Based on Bisection Sensing

The CPLA calculates the centroid coordinates of the overlapping parts through the signal coverage of the vehicle by each RSU to achieve vehicle positioning. The radius sensing method will be improved by improving the CPLA [27]. The distance between the vehicle and the RSU will be measured by dichotomy. The vehicle path prediction will be realized by Kalman filtering. The following calculation process determines the positioning coordinates of the vehicle at a given time.

1) RSU Communication Area Selection: When the RSU has the maximum communication radius $Rmax$ and the minimum communication radius $Rmin$, the RSU power adjustment can set the communication range. The RSU is set to sense the minimum communication radius of the vehicle under different communication ranges. Since flooding broadcast during RSU communication sensing increases network overhead, this method can effectively obtain a more accurate minimum communication radius of the vehicle.

As shown in Algorithm_2, R is the actual sensing radius of the OBU sensed by the RSU. When $(Rmax + Rmin)/2$ is less than R, $(Rmax + Rmin)/2$ is assigned to $Rmin$ to increase the sensing radius. Otherwise, it is assigned to $Rmax$. When $Rmax - Rmin$ is less than ε, the algorithm terminates to return to a value, $(Rmax + Rmin)/2 + \varepsilon$, slightly larger than R.

Algorithm 2 Minimum radius sensing method

while $Rmax - Rmin > \varepsilon$ **do**
  if $R > (Rmax + Rmin)/2$ **then**
    $Rmin \leftarrow (Rmax + Rmin)/2$
  else
    $Rmax \leftarrow (Rmax + Rmin)/2$
  end if
  return $(Rmax + Rmin)/2 + \varepsilon$
end while

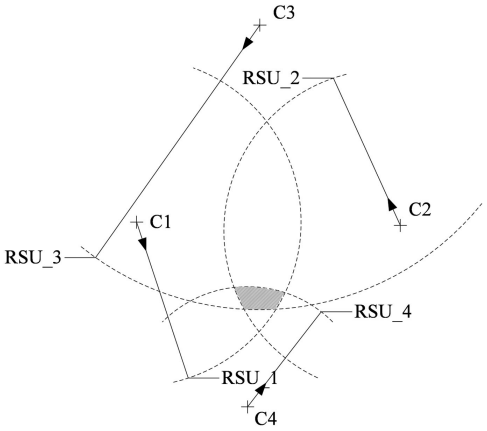

Fig. 6. Common sensing area.

2) Common Sensing Area Vertex: During the RSU flooding process, the OBU forms a common sensing area by accepting the minimum communication radius calculated by the signal strength for multiple RSUs and calculates the vertices according to the common sensing area. As shown in Fig. 6, the shaded parts are the common sensing areas of the sensing ranges of RSU_1, RSU_2, RSU_3, and RSU_4.

The OBU coordinates are calculated by the minimum sensing radius of the nearest tubular intersection RSU in each tubular cluster. RSU_1, RSU_2...RSU_n can sense that the minimum communication radius of the vehicle is R1, R2...Rn, respectively, and their corresponding center coordinates are $C_1(x_1, y_1), C_1(x_2, y_2), \ldots, C_n(x_n, y_n)$. The coordinates of the two intersection points between the two circles are (x_{pi}, y_{pi}), where $i = (1, 2, \ldots, n)$. The following equation, Equation (1), can calculate the coordinates of the vertex of the common sensing area.

$$\begin{cases} (x_{p1} - x_1)^2 + (y_{p1} - y_1)^2 = R_1 \\ (x_{p1} - x_2)^2 + (y_{p1} - y_2)^2 = R_1 \\ (x_{p2} - x_2)^2 + (y_{p2} - y_2)^2 = R_2 \\ (x_{p2} - x_3)^2 + (y_{p2} - y_3)^2 = R_2 \\ \cdots \\ (x_{pn} - x_n)^2 + (y_{pn} - y_n)^2 = R_n \\ (x_{pn} - x_1)^2 + (y_{pn} - y_1)^2 = R_n \end{cases} \tag{1}$$

As shown in Equation (2), the OBU coordinates are filtered by the relationship between the intersection point of the minimum communication radius and the other RSU sensing radius.

$$\begin{cases} \sqrt{(x_{p1} - x_3)^2 + (y_{p1} - y_3)^2} \le R_3 \\ \sqrt{(x_{p2} - x_4)^2 + (y_{p2} - y_4)^2} \le R_4 \\ \cdots \\ \sqrt{(x_{pn} - x_2)^2 + (y_{pn} - y_2)^2} \le R_2 \end{cases} \tag{2}$$

Combining the two equations, the intersection points in the minimum common sensing regions of the respective RSUs are calculated respectively as $P_i(x_{pi}, y_{pi}), i = (1, 2, \ldots, n)$, thereby obtaining the vertices of the common sensing region.

3) Calculation of Centroid Coordinates: In the CPLA, the centroid coordinate of the common sensing region is the final coordinate point, and the centroid coordinate $C(x_c, y_c)$ is obtained according to the following equation:

$$\begin{cases} x_c = (x_{p1} + x_{p2} + \cdots + x_{pn})/n \\ y_c = (y_{p1} + y_{p2} + \cdots + y_{pn})/n \end{cases} \tag{3}$$

A more accurate communication radius of the vehicle can be obtained with the minimum number of flooding times by this method. The time complexity and the area of the common sensing area can be reduced, while the accuracy of the OBU coordinates can be increased.

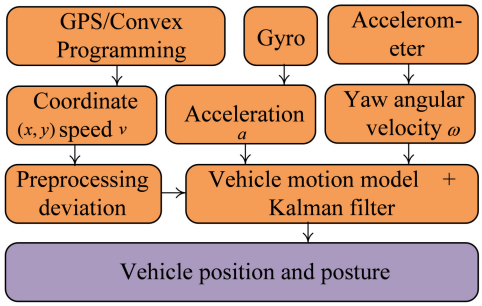

Fig. 7. Data processing flow.

B. Kalman Filter Prediction

As shown in Fig. 7, different vehicle coordinates (x, y) are obtained according to the Real Time Kinematic GPS (RTK-GPS) and the CPLA. Sensors such as the accelerometer and gyroscope can obtain the vehicle speed v and the yaw rate W, data to enhance the prediction and accuracy robustness.

As shown in Equation (4), according to the vehicle coordinates and other state information, the running state vector of moment $t - 1$ is obtained.

$$X_{(t-1)} = (x_{(t-1)}, y_{(t-1)}, v_{(t-1)}, \varphi_{(t-1)}, a_{(t-1)}, W_{(t-1)})^T, \tag{4}$$

It is assumed that the new motion state vector is obtained after Δt time from time t. Since time Δt is small, to facilitate the model establishment, the longitudinal acceleration and the yaw rate can be regarded as unchanged in the Δt time and

$W_{(T)} = \phi_{(T)}$, according to the vehicle shown in Equation (5). The law of motion obtains various parameters of the vehicle after Δt time.

$$x_{t+\Delta t} = \begin{cases} x_{(t+\Delta t)} = x_{(t)} + \Delta t \cdot v_{(t)} \cdot \cos\phi_{(t)} \\ y_{(t+\Delta t)} = y_{(t)} + \Delta t \cdot v_{(t)} \cdot \sin\phi_{(t)} \\ v_{(t+\Delta t)} = v_{(t)} + \Delta t \cdot a_{(t)} \\ \phi_{(t+\Delta t)} = \phi_{(t)} + \Delta t \cdot W_{(t)} \\ a_{(t+\Delta t)} = a_{(t)} \\ W_{(t+\Delta t)} = \phi_{(t)} \end{cases} \tag{5}$$

The state change occurs from the previous moment to the next moment, where F is the state transition matrix, and B is the control matrix. Therefore, F and B jointly control the state change of the vehicle. Equation (6) shows the state change of the motion state of the vehicle from $t-1$ to t.

$$\hat{x}_t^- = F_t \cdot \hat{x}_{t-1}^- + B_t u_t \tag{6}$$

The following equation is the transfer equation of covariance, where P is the state covariance matrix and Q is the state transition covariance matrix. The calculation of the next time state covariance matrix by two covariance matrices is shown in Equation (7).

$$P_t^- = F_t \cdot P_{t-1} \cdot F^T + Q \tag{7}$$

The following equation is the calculation of the Kalman coefficient of the observation covariance matrix. The observation matrix K_t is the Kalman coefficient. R is the observation covariance matrix, and H is the observation matrix, the true observation value of the vehicle parameter at the next moment.

$$K_t = P_t^- H^T (HP_t - H^T + R)^{-1} \tag{8}$$

Using actual observations of the vehicle parameters, the residuals of the expected observations, Kalman coefficient to estimate the vehicle motion state, prediction state covariance, and observed state covariance are combined to determine which of the two is more reliable. The estimation of the vehicle running state vector is shown in Equation (9).

$$\hat{x}_t = \hat{x}_t^- \cdot K_t (Z_t - H \cdot \hat{x}_t^-) \tag{9}$$

Finally, the noise covariance matrix is updated by using the Kalman coefficient, the observation matrix, and the covariance transfer matrix, as shown in Equation (10).

$$P_t = (I - K_t H) P_t^- \tag{10}$$

The vehicle motion model is established by the vehicle positioning information and the data from vehicular sensors. The vehicle's initial motion state is $X_{(t-1)}$, the state transition matrix is F, and the control matrix is B. The estimated value can be obtained based on the above parameters followed by the state covariance matrix P, state transition covariance matrix Q, and observation covariance matrix R.

TABLE III
MAIN PARAMETERS IN KALMAN MODEL

Parameter	Value
F	State-transition matrix
B	Control matrix, influence of outside parameter on the state
P	Deviation matrix
Q	Predictive noise covariance matrix
R	Measurement noise covariance matrix
H	Observation matrix
K_t	Kalman gain at time t
Z_t	Observation at time t
φ	Angle between longitudinal speed of car and abscissa

The state covariance matrix P is updated by Equation (7), and the Kalman coefficient K_t is obtained from the observation matrix H in Equation (8). In Equation (9), the final estimated state value is obtained by combining the predicted state covariance with the observation state covariance. Finally, the noise covariance matrix is updated by Equation (10).

The real-time coordinates of different vehicles can be obtained by RTK-GPS and CPLA and entered into the Kalman filter model. The vehicle's motion state is used to predict the target RSU of the vehicle by using multiple iterations of the estimation-observation. The received data packet is returned to the corresponding tubular cluster where the location is fixed to complete the seamless transmission of the data packet. Table III lists the main parameters in the Kalman filter model.

C. Combination of Positioning Methods

The prediction results can be calculated by combining positioning information from the CPLA based on the RSU radius sensing and the positioning data from the GPS into the Kalman prediction mode with predicted differences that can change the final result. The method of obtaining vehicle positioning information through GPS and calculating target RSU is called method GPS, and the method of obtaining vehicle positioning through CPLA and calculating target RSU is called method CP in this paper.

As shown in Fig. 8, the prediction accuracy based on the GPS is $P_{success\_GPS}$, and the prediction accuracy based on CPLA is $P_{success\_CP}$. When a vehicle switches between two specific clusters, two methods are used to generate prediction results. Then, the final prediction result by these two kinds of prediction accuracy are obtained from the different methods and are updated according to a comparison between the actual results and predicted results.

If the results calculated by the two methods are consistent, then the result is selected as the final result. If they are not, then the magnitude of the prediction accuracy of the two methods is judged, and the result produced by the method

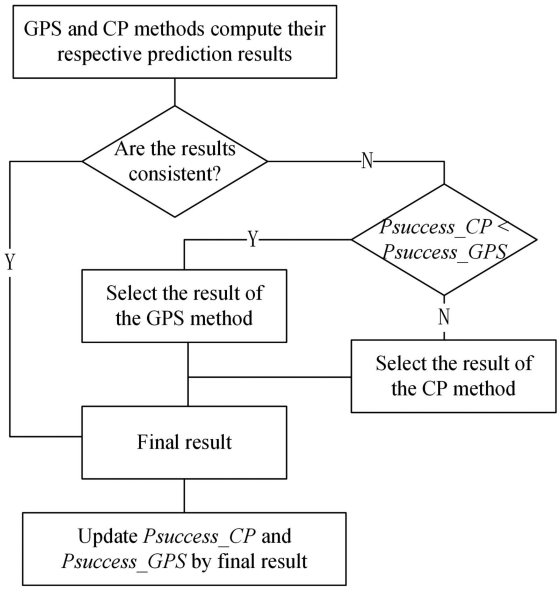

Fig. 8. Selection flowchart positioning method.

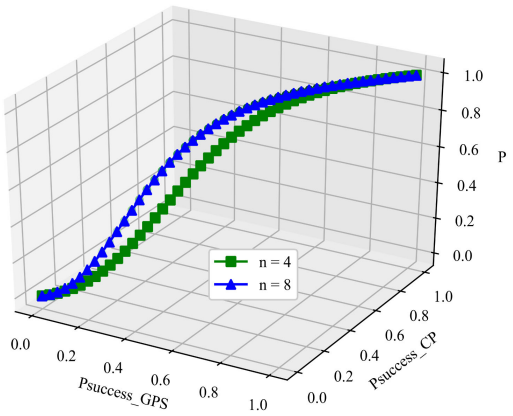

Fig. 9. Probability distribution.

with the larger prediction accuracy at the intersection is selected and used. The results after the vehicle is actually connected to the new cluster update the prediction accuracy of the two methods.

As shown in Equation (11), the number of bifurcations in an intersection is n, $n = 4$ is a common intersection scene, and $n = 8$ is an overpass traffic intersection scene. Vehicles use two methods to predict the same result in motion, and the probability that the result is correct is P.

$$P = \frac{(n-1)\cdot P_{success\_GPS}\cdot P_{success\_CP}}{n\cdot P_{success\_GPS}\cdot P_{success\_CP} - (P_{success\_GPS} + P_{success\_CP}) + 1} \tag{11}$$

As $P_{success\_GPS}$ and $P_{success\_CP}$ increase, the relationship is shown in Fig. 9.

In Equation (12),$P_{increasement}$ is an improvement value of the probability when using the method GPS and the method CP alone. These two methods can achieve correct results.

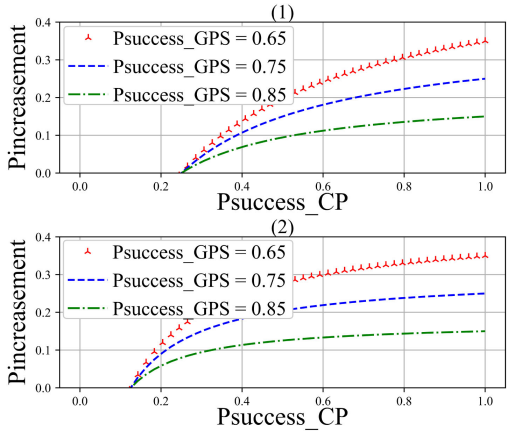

Fig. 10. Probability change.

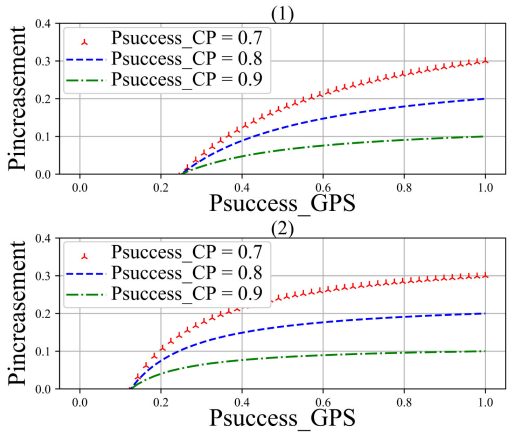

Fig. 11. Probability growth rate.

$$\begin{cases} P_{increasement} = P - P_{success\_GPS}, \\ if\ P_{success\_CP} \geq \frac{1}{n} \quad then\ P_{success\_GPS} \geq 0 \\ P_{increasement} = P - P_{success\_CP}, \\ if\ P_{success\_GPS} \geq \frac{1}{n} then\ P_{success\_CP} \geq 0 \end{cases} \tag{12}$$

When $P_{success\_GPS}$ is equal to 0.65, 0.75, and 0.85, Fig. 10 shows the probability distribution relationship between $P_{success\_CP}$ and $P_{increasement}$ at $n = 4$ and $n = 8$. From Fig. 10 (1), the accuracy growth rate is approximately 21% when CP and GPS are both 0.75. The accuracy growth rate is approximately 15% when CP and GPS are both 0.85. The increasing rate of the accuracy slows as the basic accuracy by both methods increases at the same time. When the value of $P_{success\_GPS}$ is fixed and $P_{success\_CP}$ is gradually increased, the same conclusion can be drawn from the change in the curve slope in Fig. 10.

Fig. 11 shows the change of $P_{increasement}$ when $P_{success\_CP}$ is 0.7, 0.8, and 0.9. Fig. 11 is the change of $P_{increasement}$ at the intersection and the overpass traffic intersection. In the intersection, when the minimum $P_{success\_GPS}$ is 25%, there is a probability P that the two methods have the same result. In an overpass traffic intersection, the minimum $P_{success\_GPS}$ is approximately 13%. When $P_{success\_CP}$ is 0.7 and 0.15 at an

TABLE IV
EXPERIMENTAL SIMULATION PARAMETERS

Parameter	Value
Mobility Simulator	SUMO
Map size	3200m × 3200 m
Scenario	Urban
The rate of router	20MB/s
Vehicles speeds	0-10 m/s
Number of RSUs	12
Number of Vehicles	100

overpass traffic intersection, the combination of the two methods can improve the accuracy but not at the intersection.

According to a comparison of Fig. 10 and Fig. 11, the more intersections, the faster the combination of the two methods can improve the accuracy. When the accuracy rate of one method approaches 100%, the accuracy improvement rate is lower. When the accuracy rate of one method is fixed, the probability of the two methods achieving consistent and correct results will increase with the accuracy of the other method, but the rate of increase slows.

VI. EXPERIMENTAL SIMULATION

To evaluate the performance of proposed DBPM scheme, an extensive simulation is conducted in this section. In the simulation, RSUs are set to be evenly distributed on the urban roads, and RSUs between two adjacent road intersections are set as a tubular structured cluster, and the RSU in the middle of the road section serves as the cluster-header to manage the cluster where it is located. Vehicles are randomly placed on the road with standard normal distribution which determines the moving direction of vehicles at road intersections. In general, the communication ranges of a RSU and an OBU are set to 300 m and 100 m, respectively. The road network and vehicle movements are generated in SUMO and VanetMobiSim with attribute parameters shown in Table IV.

The packet loss rate was set as the ratio of the difference between the sent interest packet and the returned data packet to the total number of interest packets sent, as shown in Equation (13).

$$P_{packet\_loss\_ratio} = \frac{Count_{Interest} - Count_{Data}}{Count_{Interest}} \tag{13}$$

In the urban area, factors such as signal occlusion, signal reflection, and superimposition of the electromagnetic wave Gaussian noise in the vehicle signal sensing process will affect the prediction result. To accurately evaluate the DBPM, the experimental scenario is assumed as ordinary intersections and overpass traffic intersections under urban road conditions. Simulation experiments are conducted with three metrics: the average hop count, packet loss ratio, and average delay.

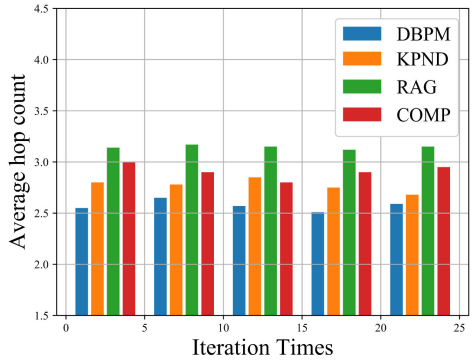

Fig. 12. Average route hops at a simple intersection.

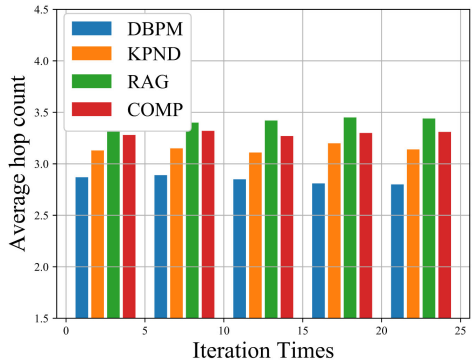

Fig. 13. Average route hops at overpass.

A. Average Hop Count

As shown in Fig. 12, at an ordinary intersection, the high-speed movement of the vehicle will cause the data packet to catch up with the moving vehicle and increase the number of data packet hops. By the quadtree search method based on the global region, the data packet hopping through the RSU relay increases the number of network hops, resulting in a higher average hop count. The DBPM combines RTK-GPS and the CPLA to generate prediction results and actively buffers data packets to the CS of the CH node in the cluster where the predicted node is located. This reduces the average hop count to some extent and solves the OBU and other factors during the steering process. Tubular clusters of frequent handovers create problems that increase the average hop count. The KPND Kalman-filter-based mobility prediction model also avoids unnecessary handover due to its predictability in the intersection steering, making the average hop count performance closer to that of the DBPM.

As shown in Fig. 13, the KPND reduces the average hop count to some extent due to the distribution of neighbor node information. The performance of the RAG using a quadtree search at complex intersections is similar to that at ordinary intersections due to its area estimation. The average hop count by the COMP at overpass traffic intersections will increase due to the complexity of the vehicle movement at the intersection. The DBPM combines the positioning information produced by the CPLA based on V2I communication to predict the target RSU when the GPS signal reception is poor. It is less affected by the GPS signal occlusion. Therefore, it has excellent performance at complex intersections.

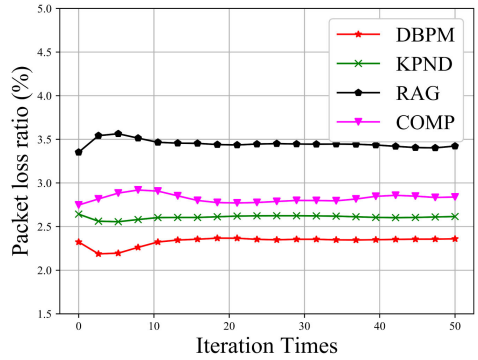

Fig. 14. Packet loss rate at a simple intersection.

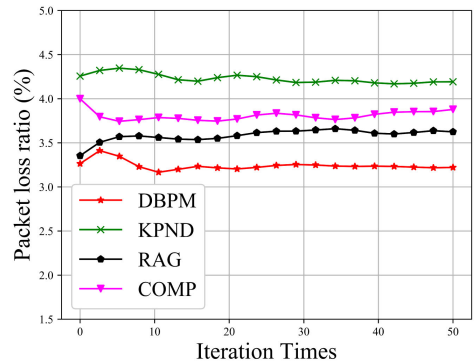

Fig. 15. Packet loss rate at an overpass.

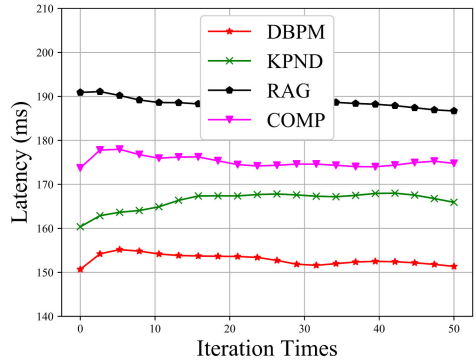

Fig. 16. Average delay at a simple intersection.

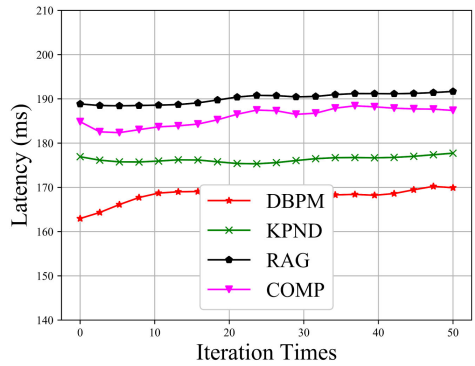

Fig. 17. Average delay at an overpass.

B. Packet Loss Ratio

As shown in Fig. 14, by the RAG in the ordinary intersection, since the RSU acts as a route relay, the randomness of the relay selection is increased to some extent during the steering of the vehicle so that the packet loss rate is high. By the COMP, the delay is affected by special road conditions at the intersection, but its cluster-based cooperative caching increases the packet hit rate to a certain extent. The KPND has a lower packet loss rate because its Kalman-based prediction model can improve the efficiency of neighbor discovery algorithms. By the DBPM, cluster-based routing can reduce the packet loss rate because of its prediction method.

As shown in Fig. 15, by the DBPM in the overpass intersection scenario, the prediction accuracy was reduced. This was affected by the GPS positioning data, which was compared with ordinary intersections. The KPND has to maintain the neighbor table in real time when its neighbor nodes are discovered. The packet loss rate increases the maintenance cost of the neighbor table at a complicated intersection. The OBU processing burden increased to some extent compared with other approaches to the packet loss rate, and the RAG performed better with its region search scheme.

C. Average Delay

As shown in Fig. 16, in the simple intersection scenario, the DBPM performs better in terms of delay in frequent handovers with a higher prediction accuracy. The RAG scheme increases latency due to its RSU selection and region search overhead.

Fig. 17 shows the delay performance of various schemes at the intersection of overpass traffic. The KPND scheme benefits from the transmission of the actual position information of the hello packet when the prediction accuracy is low, making its performance equal in both scenarios. In special road conditions such as intersections, the correlation of the vehicle's motion state is low, so the COMP based on the vehicle motion similarity will increase the data transmission delay to a certain extent.

VII. Conclusion

Aiming at relieving the problem of the reverse path breaking for data packets, which is caused by the high-speed mobility of OBUs to support better QoS in the V-NDN, a cluster routing-based data packet backhaul prediction method was proposed in this paper. This method establishes cluster routing based on the clustering structure, reduces the average hop count of the data packets, and enhances the inter-cluster handover performance by the prediction of the target RSU. At the same time, the CPLA based on bisection sensing was improved to reduce the number of flooding broadcasts in the sensing process, enhance the positioning accuracy, and improve the prediction accuracy by using a combination of two prediction schemes.

Acknowledgment

The authors also would like to thank all the anonymous reviewers for their valuable comments.

REFERENCES

[1] J. Nzouonta, N. Rajgure, G. Wang, and C. Borcea, "Vanet routing on city roads using real-time vehicular traffic information," *IEEE Trans. Veh. Technol.*, vol. 58, no. 7, pp. 3609–3626, Sep. 2009.

[2] M. Dong, K. Ota, and M. Sakai, "A novel information dissemination system for vehicle-to-rsu communication networks," in *Proc. Int. Conf. Connected Veh. Expo.*, 2013, pp. 918–919.

[3] L. Zhang *et al.*, "Named data networking," *SIGCOMM Comput. Commun. Rev.*, vol. 44, no. 3, pp. 66–73, Jul. 2014.

[4] G. Grassi, D. Pesavento, G. Pau, R. Vuyyuru, R. Wakikawa, and L. Zhang, "Vanet via named data networking," in *Proc. IEEE Conf. Comput. Commun. Workshops*, 2014, pp. 410–415.

[5] M. Chen, D. Ong Mau, Y. Zhang, T. Taleb, and V. C. Leung, "Vendnet: Vehicular named data network," *Veh. Commun.*, vol. 1, no. 4, pp. 208–213, 2014.

[6] G. Grassi *et al.*, "Acm hotmobile 2013 poster: Vehicular inter-networking via named data," *SIGMOBILE Mob. Comput. Commun. Rev.*, vol. 17, no. 3, pp. 23–24, Nov. 2013.

[7] P. K. Isa Shemsi, "Named data networking in Vanet: A survey," *Int. J. Sci. Eng. Sci.*, vol. 1, no. 11, pp. 45–49, 2017.

[8] L. Zhang *et al.*, "Named Data Networking (ndn) Project," 2012.

[9] X. Wang, Y. Li, and X. Wang, "Location-related content communications with mobility support in vehicular scenarios," *IEEE Trans. Computat. Social Syst.*, vol. 5, no. 4, pp. 918–930, Dec. 2018.

[10] C. Fang, H. Yao, Z. Wang, W. Wu, X. Jin, and F. R. Yu, "A survey of mobile information-centric networking: Research issues and challenges," *IEEE Commun. Surv. Tut.*, vol. 20, no. 3, pp. 2353–2371, Jul.–Sep. 2018.

[11] H. Li, M. Dong, and K. Ota, "Control plane optimization in software-defined vehicular ad hoc networks," *IEEE Trans. Veh. Technol.*, vol. 65, no. 10, pp. 7895–7904, Oct. 2016.

[12] V. A. Siris, X. Vasilakos, and G. C. Polyzos, "Efficient proactive caching for supporting seamless mobility," in *Proc. IEEE Int. Symp. World Wireless, Mobile Multimedia Netw.*, 2014, pp. 1–6.

[13] D. Gao, Y. Rao, C. H. Foh, H. Zhang, and A. V. Vasilakos, "Pmndn: Proxy based mobility support approach in mobile ndn environment," *IEEE Trans. Netw. Service Manag.*, vol. 14, no. 1, pp. 191–203, Mar. 2017.

[14] P. Li, T. Zhang, C. Huang, X. Chen, and B. Fu, "Rsu-assisted geocast in vehicular ad hoc networks," *IEEE Wireless Commun.*, vol. 24, no. 1, pp. 53–59, Feb. 2017.

[15] J. An, Y. Yu, J. Tang, and J. Zhan, "Fuzzy-based hybrid location algorithm for vehicle position in vanets via fuzzy kalman filtering approach," *Adv. Fuzzy Syst.*, vol. 2019, pp. 1–11, 02 2019.

[16] C. Liu, G. Zhang, W. Guo, and R. He, "Kalman prediction-based neighbor discovery and its effect on routing protocol in vehicular ad hoc networks," *IEEE Trans. Intell. Transp. Syst.*, vol. 21, no. 1, pp. 159–169, Jan. 2020.

[17] C. Anastasiades, T. Braun, and V. Siris, *Information-Centric Networking in Mobile and Opportunistic Networks*, in *Wireless Networking for Moving Objects, Lecture Notes in Computer Science*, vol. 8611, 2014, pp. 14–30.

[18] V. Sourlas, O. Ascigil, I. Psaras, and G. Pavlou, "Enhancing information resilience in disruptive information-centric networks," *IEEE Trans. Netw. Service Manag.*, vol. 15, no. 2, pp. 746–760, Jun. 2018.

[19] Y. Zhang, H. Zhang, and L. Zhang, "Kite: A mobility support scheme for ndn," in *Proc. 1st ACM Conf. Inf.-Centric Netw. (ACM-ICN '14),* 2014, pp. 179–180.

[20] N. Abani, T. Braun, and M. Gerla, "Proactive caching with mobility prediction under uncertainty in information-centric networks," in *Proc. 4th ACM Conf. Inf.-Centric Netw. (ICN '17),* 2017, pp. 88–97.

[21] M. Amadeo, G. Ruggeri, C. Campolo, and A. Molinaro, "Iot services allocation at the edge via named data networking: From optimal bounds to practical design," *IEEE Trans. Netw. Service Manag.*, vol. 16, no. 2, pp. 661–674, Jun. 2019.

[22] W. Huang, T. Song, Y. Yang, and Y. Zhang, "Cluster-based cooperative caching with mobility prediction in vehicular named data networking," *IEEE Access*, vol. 7, pp. 23 442–23 458, 2019.

[23] D. Blatt and A. O. Hero, "Energy-based sensor network source localization via projection onto convex sets," *IEEE Trans. Signal Process.*, vol. 54, no. 9, pp. 3614–3619, Sep. 2006.

[24] R. Hou, Y. Chang, and L. Yang, "Multi-constrained qos routing based on pso for named data networking," *IET Commun.*, vol. 11, no. 8, pp. 1251–1255, 2017.

[25] H. Khelifi *et al.*, "Named data networking in vehicular ad hoc networks: State-of-the-art and challenges," *IEEE Commun. Surv. Tut.*, vol. 22, no. 1, pp. 320–351, Jan.–Mar. 2020.

[26] T. Küçükdeniz, A. Baray, K. Ecerkale, and Şakir Esnaf, "Integrated use of fuzzy c-means and convex programming for capacitated multi-facility location problem," *Expert Syst. with Appl.*, vol. 39, no. 4, pp. 4306–4314, 2012.

[27] Y. E. Juan, Y. Y. Chen, M. Wang, and N. I. Ying-Bo, "Optimized convex localization algorithm using multiple communication radius and angle correction," *Comput. Ence*, vol. 46, no. 6, pp. 320–351, 2019.

Rui Hou (Member, IEEE) received the Ph.D. degree from the Huazhong University of Science and Technology, Wuhan, China, in 2006. He is currently a Professor with the College of Computer Science, South-Central University for Nationalities, Wuhan, China. He was sponsored by the Chinese Scholarship Council as a National Senior Visiting Scholar, and conducted research with Laboratory of Signaling, Communications, and Networking, Department of ECE, Colorado State University, Fort Collins, CO, USA, from 2014 to 2015. He has authored or coauthored more than 100 papers in international publications. His main research interests include computer network architecture, optical switching, and wireless sensor networks. He is also Members of CCF and IEICE.

Shuo Zhou is currently working toward the M. Eng. with the College of Computer Science, South-Central University for Nationalities, Wuhan, China. Her research interest include vehicular named data networking.

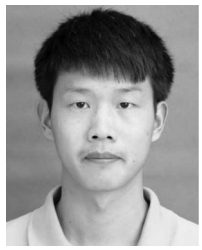

Yong Zheng is currently working toward the M.Eng. with the College of Computer Science, South-Central University for Nationalities, Wuhan, China. His research interest include artificial intelligence in information-centric networking.

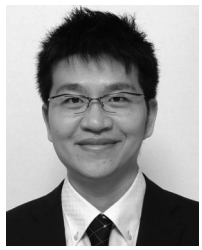

Mianxiong Dong (Member, IEEE) received the B.S., M.S., and Ph.D. degrees in computer science and engineering from The University of Aizu, Aizuwakamatsu, Japan. He is currently the Vice President and youngest ever Professor with the Muroran Institute of Technology, Muroran, Japan. He was a JSPS Research Fellow with the School of Computer Science and Engineering, The University of Aizu, and was a Visiting Scholar with BBCR Group, University of Waterloo, Waterloo, ON, Canada, supported by JSPS Excellent Young Researcher Overseas Visit Program from April 2010 to August 2011. He was selected as a Foreigner Research Fellow (a total of three recipients all over Japan) by NEC C&C Foundation in 2011. He was the recipient of IEEE TCSC Early Career Award 2016, IEEE SCSTC Outstanding Young Researcher Award 2017, The 12th IEEE ComSoc Asia-Pacific Young Researcher Award 2017, Funai Research Award 2018 and NISTEP Researcher 2018 (one of only 11 people in Japan) in recognition of significant contributions in science and technology. He is Clarivate Analytics 2019 Highly Cited Researcher (Web of Science).

Kaoru Ota (Member, IEEE) was born in Aizu-Wakamatsu, Japan. She received the B.S. degree in computer science and engineering from The University of Aizu, Aizuwakamatsu, Japan in 2006, the M.S. degree in computer science from Oklahoma State University, Stillwater, OK, USA in 2008, and the Ph.D. degree in computer science and engineering from The University of Aizu, in 2012. She is currently an Associate Professor and Ministry of Education, Culture, Sports, Science and Technology Excellent Young Researcher with the Department of Sciences and Informatics, Muroran Institute of Technology, Muroran, Japan. From March 2010 to March 2011, she was a Visiting Scholar with the University of Waterloo, Waterloo, ON, Canada. From April 2012 to April 2013, she was a Japan Society of the Promotion of Science Research Fellow with Tohoku University, Sendai, Japan. He was the recipient of IEEE TCSC Early Career Award 2017, The 13th IEEE ComSoc Asia-Pacific Young Researcher Award 2018, and 2020 N2Women: Rising Stars in Computer Networking and Communications. She is Clarivate Analytics 2019 Highly Cited Researcher (Web of Science).

Deze Zeng (Member, IEEE) received the Ph.D. degree from the University of Aizu, Aizuwakamatsu, Japan. His current research interests include wireless sensor networks, network function virtualization, software-defined networking, cloud computing, and edge computing. He is on the Editorial Boards of Elsevier *Journal of Network and Computer Applications* and *Frontiers of Computer Science*.

Jiangtao Luo (Senior Member, IEEE) received the Ph.D. degree from the Chinese Academy of Science, Beijing, China, in 1998. He is currently a Professor with the Electronic Information and Networking Research Institute, Chongqing University of Posts and Telecommunications, Chongqing, China. He has authored more than 100 papers and holds 21 patents in these fields. His major research interests are network data mining, urban computing, and future internet architecture. He is also an ACM Member. He was the recipient of the Chinese State Award for Scientific and Technological Progress in 2011, the Chongqing Provincial Award for Scientific and Technological Progress in 2007 and 2010, and the Chongqing Science and Technology Award for Youth in 2010.

Maode Ma (Senior Member, IEEE) received the Ph.D. degree in computer science from Hong Kong University of Science and Technology, Hong Kong, in 1999. He is currently an Associate Professor with the School of Electrical and Electronic Engineering, Nanyang Technological University, Singapore. He has extensive research interests including network security and wireless networking. He has more than 400 international academic publications including approximately 200 journal papers and more than 200 conference papers. He has delivered approximately 70 keynote speeches at various international conferences. He was the Conference Chair for more than 100 international conferences. He is currently the Editor-in-Chief of the *Journal of Communications*, *International Journal of Computer and Communication Engineering*, and *International Journal of Electronic Transport*. He is also the Senior Editor and an Associate Editor for other five international academic journals. He is a Senior Member of IEEE Communication Society and IEEE Education Society, and a Member of ACM. He is the Secretary of the IEEE Singapore Section and Chair of the ACM, Singapore Chapter. From 2013 to 2016, he was an IEEE Communication Society Distinguished Lecturer.